Inorg. Chem. **2006**, *45*, 7943–7946

$KCaEr_2CuS_5$: A New Pentanary Rare-Earth Layered Chalcogenide without Substitutional Disorder

Hui-Yi Zeng,[†,‡] HansJürgen Mattausch,[‡] Arndt Simon,[‡] Fa-Kun Zheng,[†] Zhen-Chao Dong,*[,†,§] Guo-Cong Guo,*[,†] and Jin-Shun Huang[†]

State Key Laboratory of Structural Chemistry, Fujian Institute of Research on the Structure of Matter, Chinese Academy of Sciences, Fuzhou, Fujian 350002, P. R. China, Max Planck Institute for Solid State Research, Heisenbergstrasse 1, D-70569 Stuttgart, Germany, and Hefei National Laboratory for Physical Sciences at Microscale, University of Science and Technology of China, Hefei, Anhui 230026, P. R. China

Received May 24, 2006

A new pentanary rare-earth chalcogenide without substitutional disorder, $KCaEr_2CuS_5$, was obtained from reaction of the Er–Ca–Cu–S precursor with KBr flux by either a two-step flux method or a direct reaction of the mixture of the binary components ($1Cu_2S:2Er_2S_3:3CaS$) with excess KBr as flux. $KCaEr_2CuS_5$ crystallizes in the orthorhombic space group *Cmcm* (No. 63) with $a = 3.9327(5)$ Å, $b = 13.410(2)$ Å, $c = 17.042(2)$ Å, $V = 898.8(3)$ Å^3, $Z = 4$, $R = 0.0632$, and $R_w = 0.0627$. The $KCaEr_2CuS_5$ structure consists of four different building units: ErS_6 octahedra, CaS_6 octahedra, CuS_4 tetrahedra, and KS_6 trigonal prisms; it is characterized by $^2_\infty[Er_2CuS_5]^{3-}$ layers that are formed by the interconnection of double ErS_6 octahedral chains with CuS_4 tetrahedral chains in the *a*–*c* plane. K^+ and Ca^{2+} cations are located in the cavities defined by S^{2-} anions between the $^2_\infty[Er_2CuS_5]^{3-}$ layers. $KCaEr_2CuS_5$ is a semiconductor with an estimated band gap of 2.4 eV and shows a Curie–Weiss paramagnetic behavior in the 5–300 K range.

Introduction

Multinary rare-earth chalcogenides have attracted much attention both for their varieties of structural features and for their potential applications as luminescence, magnetooptical, and infrared materials.[1,2] It is widely realized that during the synthesis and crystal growth via flux methods, occasional inclusion of flux elements in the final product is inevitable and often leads to unexpected and interesting new structures. Serendipitously, during our effort to explore new rare-earth cuprates, we obtained a new pentanary rare-earth layered sulfide, $KCaEr_2CuS_5$, by a two-step synthetic route. The same phase was also successfully prepared subsequently by a direct reaction of the binary sulfides Cu_2S, Er_2S_3, and CaS with excess KBr as reactive flux.

Reactive halide flux methods have produced many interesting rare-earth chalcogenides.[3−19] However, pentanary rare-earth chalcogenides without oxygen are rather rare and limited to mainly $K_{0.5}Ba_{0.5}DyCu_{1.5}Te_3$,[4] $LaCa_2GeS_4Cl_3$,[7] $La_{3-x}Ce_x(SiS_4)_2I$ ($0 < x < 1$),[20] $LaCeSbS_5Br$,[21] and $(La_{0.5}Ce_{0.5})SbS_2Br_2$.[22] $K_{0.5}Ba_{0.5}DyCu_{1.5}Te_3$ is the first example

* To whom correspondence should be addressed. E-mail: zcdong@ustc.edu.cn (Z.-C.D.); gcguo@fjirsm.ac.cn (G.-C.G.).
† Chinese Academy of Sciences.
‡ Max Planck Institute for Solid State Research.
§ University of Science and Technology of China.

(1) Flahaut, J. In Gschneidner, K. A., Jr.; Eyring, L. R., Eds.; *Handbook on the Physics and Chemistry of Rare Earth*; North-Holland Publishing Company: Amsterdam, 1979; Vol. 4, pp 1−88 and references therein.
(2) Wu, P.; Ibers, J. A. *J. Alloys Compd.* **1995**, 229, 206−215 and references therein.
(3) Bucher, C. K.; Hwu, S.-J. *Inorg. Chem.* **1994**, *33*, 5831−5835.
(4) Huang, F. Q.; Choe, W.; Lee, S.; Chu, J. S. *Chem. Mater.* **1998**, *10*, 1320−1326.
(5) Folchnandt, M.; Schleid, T. *Z. Anorg. Allg. Chem.* **1998**, 624, 1595−1600.
(6) Kim, S. J.; Park, S. J.; Yun, H.; Do, J. *Inorg. Chem.* **1996**, *35*, 5283−5289.
(7) Gitzendanner, R. L.; DiSalvo, F. J. *Inorg. Chem.* **1996**, *35*, 2623−2626.
(8) Zeng, H.-Y. Ph.D. Thesis, Fujian Institute of Research on the Structure of Matter, Chinese Academy of Sciences, Fujian, P. R. China, 1998.
(9) Zeng, H.-Y.; Mao, J.-G.; Chen, J.-T.; Dong, Z.-C.; Guo, G.-C.; Huang, J.-S. *J. Alloys Compd.* **2002**, *336* (1/2), 148−153.
(10) Tranchitella, L. J.; Fettinger, J. C.; Eichhorn, B. W. *J. Solid State Chem.* **1999**, *147*, 592−600.
(11) Tougait, O.; Ibers, J. A. *Inorg. Chem.* **2000**, *39*, 6136−6138.
(12) Hartenbach, I.; Schleid, T. *Z. Anorg. Allg. Chem.* **2002**, *628*, 1327−1331.
(13) Lissner, F.; Hartenbach, I.; Schleid, T. *Z. Anorg. Allg. Chem.* **2002**, *628*, 1552−1555.
(14) Hartenbach, I.; Schleid, T. *J. Solid State Chem.* **2003**, *171*, 382−386.
(15) Hartenbach, I.; Schleid, T. *Z. Anorg. Allg. Chem.* **2005**, *631*, 1365−1370.
(16) Komm, T.; Schleid, T. *Z. Anorg. Allg. Chem.* **2006**, *632*, 42−48.
(17) Mills, A. M.; Ruck, M. *Inorg. Chem.* **2006**, *45*, 5172−5278.
(18) Hartenbach, I.; Schleid, T. *J. Alloys Compds.* **2006**, *418*, 68−72.
(19) Hartenbach, I.; Schleid, T. *J. Alloys Compds.* **2006**, *418*, 95−100.

10.1021/ic060907j CCC: $33.50
Published on Web 08/09/2006

containing four metallic elements, but this and all other compounds listed above are disordered substitutionally. Here, we present the synthesis, single-crystal structure and optical and magnetic properties of $KCaEr_2CuS_5$.

Experimental Section

Synthesis. All starting materials were used as received. A mixture of Er_2S_3 (99.9%, 0.277 mmol), CaS (99.95%, 0.277 mmol), Cu (99.999%, 0.554 mmol), and S (99.999%, 0.555 mmol) was ground thoroughly under a N_2 gas atmosphere in a drybox and then pressed into a pellet, which was subsequently sealed in an evacuated, fused silica ampule. It was heated to 750 °C in a furnace at a rate of 4 °C/h and kept there for 24 h; the temperature was then raised at 10 °C/h to 1000 °C for 120 h, and finally, the furnace power was switched off.

The precursor from the first-step solid-state reaction was mixed with an excess amount of KBr flux (99.9%, 0.88 g). After regrinding, repelletizing, and resealing, we heated the precursor-flux mixture at a rate of 10 °C/h to 800 °C; the mixture was equilibrated at this temperature for 2 weeks prior to slow cooling (~3 °C/h) to room temperature. Light yellow, transparent, needlelike single crystals were manually selected from the residual after excess KBr had been washed away with distilled water. These $KCaEr_2CuS_5$ crystals are very stable in air.

Semiquantitative energy dispersive analysis by X-ray (EDAX) analysis with an ETEC AutoProbe Tracor-Northern TN-5400 energy disperse X-spectrometer confirmed the presence of K, Ca, Er, Cu, and S with a molar ratio around 1:1:2:1:5 in the crystal that was selected for X-ray diffraction analysis.

Single crystals of $KCaEr_2CuS_5$ could be obtained repeatedly either by the above two-step flux route or by the reaction of Cu_2S, Er_2S_3, and CaS with excess KBr. To obtain a sufficient amount of pure $KCaEr_2CuS_5$ phase for property measurements, we explored in more detail the rational syntheses based on the direct reaction of binary components with excess KBr as flux. The highest yield achieved so far is 65%, estimated on the basis of Cu, and resulted from a reaction in a Cu_2S:$2Er_2S_3$:3CaS molar ratio with excess KBr (Cu_2S:$2Er_2S_3$:3CaS charge: KBr = 1:2 by weight). It mixture was thermally treated as follows: The mixture was equilibrated at 1000 °C for 180 h in an alumina crucible jacketed in an evacuated silica tube and cooled slowly to 700 °C over 90 h. Excess KBr flux and any other soluble compound(s) were removed by washing the reaction mixture with distilled water at room temperature using a suction filtration technique. The homogeneity of the as-prepared sample was confirmed by powder X-ray diffraction and energy dispersive spectroscopy. No binary or ternary compound was detected.

Crystallography. (a) Single-Crystal Diffraction. A crystal with approximate dimensions of $0.10 \times 0.01 \times 0.01$ mm^3 was selected for data collection. Intensity data were collected by the $\omega-2\theta$ scan mode on an Enraf−Nonious CAD4 diffractometer with graphite-monochromated Mo Kα radiation ($\lambda = 0.71073$ Å). The unit-cell parameters were determined by least-squares refinement of 25 reflections with $12° < 2\theta < 30°$. A total of 1625 reflections were measured in the range $2° < 2\theta < 80°$, of which 713 reflections with $I > 3\sigma(I)$ were used for structure refinements. Intensities were corrected for Lorentz polarization and for absorption using the ψ-scan technique. The structure was solved by direct methods and difference Fourier synthesis, refined by full-matrix squares techniques. Final refinements for 35 variables led to the agreement factors $R = 0.0632$, $R_w = 0.0627$. The maximal residual is 2.28 Å from the Er atom and 2.32 Å from the K atom position, whereas the lowest residual is 2.55 Å from Er, 2.08 Å from Ca, and 1.95 Å from the S(2) atom position. All calculations were performed using the MolEN package.[23] Some details of the data collection and refinements are summarized in Table 1, the positional coordinates and isotropic equivalent thermal parameters are given in Table 2, and important bond distances and angles are given in Table 3. Further details of the crystal structure investigation(s) can be obtained from the Fachinformationszentrum Karlsruhe, 76344 Eggenstein-Leopoldshafen, Germany, (fax: (49) 7247-808-666; e-mail: crysdata@fiz-karlsruhe.de) on quoting the depository number CSD-412517.

Table 1. Crystal Data and Experimental Details for $KCaEr_2CuS_5$

	$KCaEr_2CuS_5$
fw	637.56
cryst syst	orthorhombic
space group	*Cmcm* (No. 63)
cell params	
a (Å)	3.9327(5)
b (Å)	13.410(2)
c (Å)	17.042(2)
V (Å^3)	898.8(3)
Z	4
F(000)	1136
D_{calcd} (mg/m^3)	4.17
T (K)	293
cryst dimension (mm^3)	$0.10 \times 0.01 \times 0.01$
cryst color, shape	yellow, needle
radiation (graphite-monochromated)	Mo Kα ($\lambda = 0.71073$ Å)
linear abs coeff (mm^{-1})	23.18
T_{min}/T_{max}	0.911/1.000
decay (%)	6.0
scan type	$\omega-2\theta$, $1.00 + 0.35\tan(\theta)$
scan range	$2° \le 2\theta \le 80°$
scan speed (deg min^{-1})	≤16.48/3
cell measurement	25, $14° < \theta < 15°$
θ_{max} (deg)	40.0
h, *k*, *l* range	$0 \le h \le 7$, $-24 \le k \le 0$, $0 \le l \le 30$
no. of total data points	1625
no of unique data points with $I > 3\sigma(I)$	713
R_{int}	0.0434
no. of variables	35
S,[a] R^b/R_w[c]	1.05, 0.0632/0.0627
weighting scheme	$W = 1/(\sigma^2(F))$
$(\Delta/\sigma)_{max}$	0.0001
high/low residual (e Å^{-3})	5.27/−4.78

[a] $S = [\sum w(|F_o| - |F_c|)^2/(N_{obs} - N_{var})]^{1/2}$ [b] $R = \sum||F_o| - |F_c||/\sum|F_o|$. [c] $R_w = [\sum(|F_o| - |F_c|)^2/\sum w|F_o|^2]^{1/2}$.

Table 2. Positional and Thermal Parameters with ESD for $KCaEr_2CuS_5$

atom	Wyckoff site	site occupancy	*x*	*y*	*z*	$U_{(eq)}$[a] (Å^2)
Er	8*f*	0.99(2)	0	0.27021(8)	0.39703(6)	0.0067(1)
Cu	4*c*	1	0	0.7961(3)	0.25	0.0110(8)
Ca	4*a*	1.01(3)	0	0	0	0.007(1)
K	4*c*	1	0	0.5235(5)	0.25	0.018(2)
S(1)	4*c*	1	0	0.2002(6)	0.25	0.009(1)
S(2)	8*f*	1	0	0.8977(4)	0.1395(3)	0.010(1)
S(3)	8*f*	1	0	0.6425(4)	0.0471(3)	0.006(1)

[a] $U_{(eq)}$ is defined as one-third of the trace of the orthogonalized U_{ij} tensor.

(20) Riccardi, R.; Gout, D.; Gauthier, G.; Guillen, F.; Jobic, S.; Garcia, A.; Huguenin, D.; Macaudiere, P.; Fouassier, C.; Brec, R. *J. Solid State Chem.* **1999**, *147*, 259−268.
(21) Gout, D.; Jobic, S.; Evain, M.; Brec, R. *Solid State Sci.* **2001**, *3*, 223−234.
(22) Gout, D.; Jobic, S.; Evain, M.; Brec, R. *J. Solid State Chem.* **2001**, *158*, 218−226.
(23) Fair, C. K. *MolEN. An Interactive Intelligent System for Crystal Structure Analysis*; Enraf−Nonius: Delft, The Netherlands, 1990.

Table 3. Selected Bond Distances Lengths for $KCaEr_2CuS_5$

bond	distance (Å)	bond	distance (Å)
Er−S(1) (×1)	2.676(3)	Cu−S(1) (×2)	2.349(5)
Er−S(2) (×2)	2.679(4)	Cu−S(2) (×2)	2.325(6)
Er−S(3) (×1)	2.813(5)	K−S(1) (×2)	3.079(8)
Er−S(3) (×2)	2.776(4)	K−S(2) (×4)	3.204(6)
Ca−S(2) (×2)	2.744(6)	K−S(3) (×2)	3.808(6)
Ca−S(3) (×4)	2.857(4)		

(b) X-ray Powder Diffraction. The powder diffraction pattern was recorded on a STOE Stadi P powder diffractometer (Stoe, Darmstadt, Germany), using germanium-monochromatized Cu Kα radiation (λ = 1.54057 Å). The observed powder pattern was in good agreement with that calculated using the STOE WinXPOW package.[24] Indexing and refining 29 diffraction peaks in the range $5° \le 2\theta \le 65°$ in space group *Cmcm* gave the following cell parameters: a = 3.9333(25) Å, b = 13.462(6) Å, and c = 17.056(8) Å.

Magnetic Susceptibility. The dc magnetic susceptibility (χ = M/H) measurements on a powdered sample (0.11421 g) were performed on a Quantum Design PPM-9T magnetometer at a field of 5000 Oe cooling from 300 to 5 K. The raw data were corrected for the susceptibility of the container and for the diamagnetic contribution from the atomic cores of K^+, Ca^{2+}, Cu^+, Er^{3+}, and S^{2-} (-2.273×10^{-4} emu/mol) from Pascal increments.[25]

UV−Vis Diffuse Reflectance Spectroscopy. The optical diffuse reflectance spectrum of powdered $KCaEr_2CuS_5$ was measured at room temperature using a Perkin−Elmer Lambda 900 UV−vis spectrophotometer equipped with an integrating sphere attachment and $BaSO_4$ as reference. The absorption spectrum was calculated from the reflection spectrum via the Kubelka−Munk function: $\alpha/S = (1 - R)^2/2R$, in which α is the absorption coefficient, S is the scattering coefficient, and R is the reflectance.[26]

Infrared Spectroscopy. IR spectra were recorded on a Nicolet Magna 750 Fourier transform infrared spectrometer equipped with a DTGS detector using two references, a KBr disk in the 4000−400 cm^{-1} region at a resolution of 4.0 cm^{-1} with 32 scans and a CsI disk in the 600−100 cm^{-1} region at a resolution of 4 cm^{-1} with 72 scans under a dried air flow.

Results and Discussion

$KCaEr_2CuS_5$ is the first example of a pentanary rare earth chalcogenide without substitutional disorder, the site occupancies of Er (8*f* site) and Ca (4*a* site) are 100% with statistical errors (see the refined occupation factors for Ca and Er in Table 2). $KCaEr_2CuS_5$ contains four types of building units in the structure, octahedral ErS_6 and CaS_6, tetrahedral CuS_4, and trigonal prismatic KS_6, as shown in Figure 1.

The structure is characterized by $^2_\infty[Er_2CuS_5]^{3-}$ layers that are formed by the interconnection of double ErS_6 octahedral chains with CuS_4 tetrahedral chains in the $a-c$ plane. ErS_6 octahedra each share opposite [S(2)−S(3)] edges along the a direction, forming $^1_\infty[ErS(1)S(2)_{2/2}S(3)_{1+2/2}]$ chains; each pair of $^1_\infty[ErS(1)S(2)_{2/2}S(3)_{1+2/2}]$ chains is further condensed by sharing one side of octahedral edges in a zigzag manner via S(3)−S(3) (Figure 2). The CuS_4 tetrahedra are also condensed into a corner-sharing $^1_\infty[CuS(1)_{2/2}S(2)_2]$ chain along the a axis. These double-

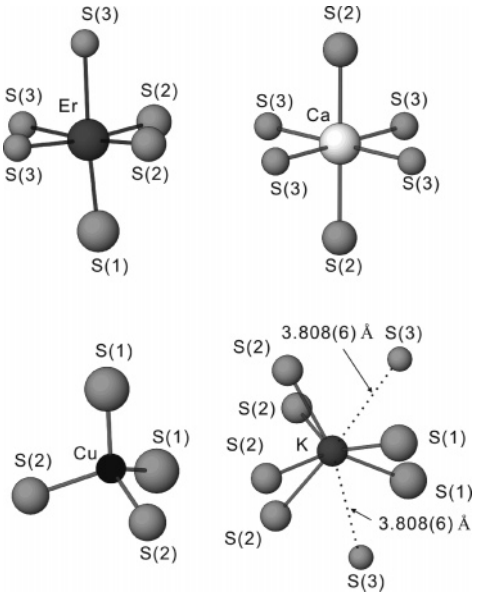

Figure 1. Coordination geometries of octahedral ErS_6, CaS_6, tetrahedral CuS_4, and bicapped trigonal prismatic KS_6.

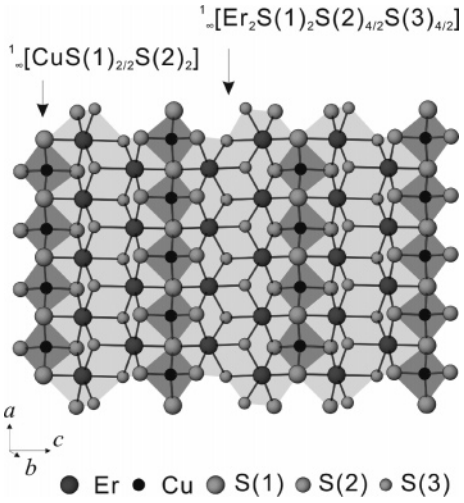

Figure 2. Projection of a $^2_\infty[Er_2CuS_5]^{3-}$ slab on the $a-c$ plane with double-octahedral $^1_\infty[Er_2S(1)_2S(2)_{4/2}S(3)_{4/2}]$ (gray) chains and tetrahedral $^1_\infty[CuS(1)_{2/2}S(2)_2]$ (black) chains. The chains are emphasized.

octahedral $^1_\infty[Er_2S(1)_2S(2)_{4/2}S(3)_{4/2}]$ chains are connected into a $^2_\infty[Er_2CuS_5]^{3-}$ layer via corner-sharing of S(1), with Cu atoms filling the tetrahedral sites. In other words, the $KCaEr_2CuS_5$ structure may be viewed as a layered structure composed of $^2_\infty[Er_2CuS_5]^{3-}$ slabs in which chains of corner-sharing tetrahedral $^1_\infty[CuS(1)_{2/2}S(2)_2]$ units connect neighboring double-octahedral $^1_\infty[Er_2S(1)_2S(2)_{4/2}S(3)_{4/2}]$ chains, and vice versa (Figure 2).

The $^2_\infty[Er_2CuS_5]^{3-}$ slabs are stacked along the b direction with K^+ and Ca^{2+} cations located in different cavities between the layers (Figure 3). Figure 3 is a projection of the crystal structure showing how ErS_6 octahedra and CuS_4 tetrahedra are connected into $^2_\infty[Er_2CuS_5]^{3-}$ layers, shaping the one-dimensional channels for K^+ and Ca^{2+} cations along the a direction. The Ca atoms are surrounded octahedrally

(24) *STOE WinXPOW*, version 1.2; STOE & Cie GmbH: Darmstadt, Germany, 2001.
(25) Selwood, P. W. *Magnetochemistry*, 2nd ed.; Interscience Publishers: New York, 1956, p 70.
(26) Kortüm, G. *Reflectance Spectroscopy*; Springer−Verlag: New York, 1969.

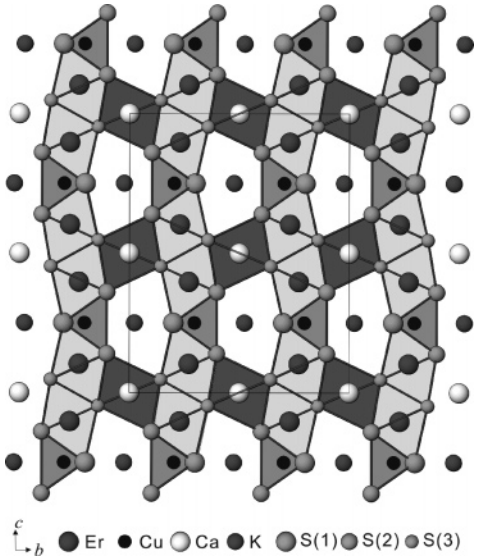

Figure 3. Projection of the crystal structure of $KCaEr_2CuS_5$ along the *a* direction. The channels of ErS_6 octahedra (gray) and CuS_4 tetrahedra (black) forming layers along [100] are emphasized. Between the layers, the Ca^{2+} and K^+ ions are localized.

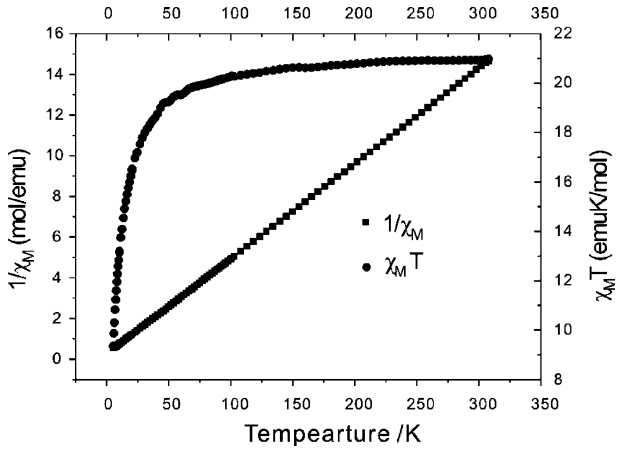

Figure 4. Temperature dependence of the dc molar magnetic susceptibility for $KCaEr_2CuS_5$, measured in an applied field of 5000 Oe.

(distorted) by 6 S atoms with Ca−S(2) (×2) in a distance of 2.744(6) Å and Ca−S(3) (×4) of 2.857(4) Å. The K atoms in the channels are each surrounded by eight S (2 × S(1), 4 × S(2), 2 × S(3)) atoms, forming bicapped trigonal prisms.

In $KCaEr_2CuS_5$, the Er−S distances range from 2.676(3) to 2.813(5) Å, with an average value of 2.733 Å, consistent with the sum of ionic radii (2.730 Å).[27] The Cu−S distances vary from 2.325(6) to 2.349(5) Å, in agreement with those (2.339(2)−2.392(2) Å) in $BaErCuS_3$.[28] The Ca−S distance of 2.820 Å is very close to the sum of the Shannon radii for six-coordinated Ca^{2+} and S^{2-} (2.84 Å).[27] If two distant S(3) atoms (3.808(6) Å away) are not included, the K−S distances ranging from 3.079(8) to 3.204(6) Å are comparable to those in KGd_2CuS_4 (3.119(2)−3.253(2) Å).[29]

Figure 4 shows the temperature dependence of the susceptibility of $KCaEr_2CuS_5$ measured from 300 down to 5 K. A fit with $\chi_M = C/(T - \theta) + \chi_0$ to all data reveals a Curie−Weiss behavior with Curie constant $C = 22.13(2)$ emu K/mol and Weiss temperature $\theta = -6.86(1)$ K, leading to an effective magnetic moment of 13.30 μ_B (per $KCaEr_2CuS_5$). The background susceptibility χ_0 is −0.0035(3) emu/mol, which is negligible compared with the room-temperature molar susceptibility χ_M (300 K) = 0.0686 emu/mol.

In the structure of $KCaEr_2CuS_5$, the Er ions are well-separated (the shortest Er−Er distance is 3.9327(5) Å) and can be treated as isolated magnetic centers. Thus each isolated Er ion in $KCaEr_2CuS_5$ has a Curie constant of 22.13(2)/2 = 11.07(1) emu K/mol and an effective magnetic moment of 9.41(1) μ_B, which is in good agreement with the 9.59 μ_B predicted for the ground-state Er^{3+} ($^4I_{15/2}$) according to $\mu_{eff} = g[J(J + 1)]^{1/2}$. $KCaEr_2CuS_5$ is valence-precise according to $K^+Ca^{2+}Er_2^{6+}Cu^+S_5^{10-}$ and expected to be a semiconductor. Indeed, in addition to those narrow spectral lines that arise from the f−f transitions of Er^{3+}, the optical reflectance measurements indicate an estimated band gap of 2.4 eV for $KCaEr_2CuS_5$, consistent with its yellow color.

The very weak absorption band around 3500 cm^{-1} in the mid-IR spectrum of $KCaEr_2CuS_5$ is attributed to the trace water absorbed from air by the sample. The solid-state far-IR spectrum of $KCaEr_2CuS_5$ shows the following peaks: 393 (w), 339 (s), 326 (m), 291(s), 260 (s), 226 (s), 214 (s) cm^{-1}. Peaks at 291−403 cm^{-1} are tentatively assigned to the Cu−S vibrations in previous reports on $KCuCe_2S_6$, $KCuLa_2S_6$, and $CsCuCe_2S_6$.[30] The bands below 250 cm^{-1} are presumably due to K−S, Ca−S, and Er−S bonds.

Conclusion

A novel pentanary rare-earth layered chalcogenide, $KCaEr_2CuS_5$, has been prepared by the reactive flux method. The $KCaEr_2CuS_5$ structure is built from ErS_6, CaS_6 octahedra, CuS_4 tetrahedra, and KS_6 trigonal prisms. The compound illustrates again a common feature in the rare-earth−transition-metal chalcogenides: Although the basic building units are the same or similar, novel and different structures may occur because of the different packing schemes of these MQ_n polyhedra. Consistent with the isolated Er^{3+} centers in the structure, the phase shows a Curie−Weiss paramagnetic behavior in the 5−300 K range. $KCaEr_2CuS_5$ is a semiconductor with an estimated band gap of 2.4 eV.

Acknowledgment. The authors thank Claudia Kamella and Viola Duppel for the EDX analysis. This work was partially supported by the NSFC (20425104, 10574117) and the NSF of Fujian Province (Z0513020) and CAS (KJCX2-SW-h05).

Note Added after ASAP Publication. This article was released ASAP on August 9, 2006 with refs 25 and 26 transposed. The correct version was posted on August 15, 2006.

Supporting Information Available: Crystallographic data in CIF format, optical absorption spectrum transformed from diffuse reflectance data, Far-IR data (600−200 cm^{-1}). This material is available free of charge via the Internet at http://pubs.acs.org.

IC060907J

(27) Shannon, R. D. *Acta Crystallogr., Sect. A* **1976**, *32*, 751−767.
(28) Wu, P.; Christuk, A. E.; Ibers, J. A. *J. Solid State Chem.* **1994**, *110*, 337−344.
(29) Stoll, P.; Dürich, P.; Näther, C.; Bensch, W. *Z. Anorg. Allg. Chem.* **1998**, *624*, 1807−1810.
(30) Sutorik, A. C.; Albritton-Thomas, J.; Hogan, T.; Kannewurf, C. R.; Kanatzidis, M. G. *Chem. Mater.* **1996**, *8*, 751−61.